APPLICATION OF MACHINE LEARNING METHODS TO FORECAST PETROPHYSICAL PROPERTIES IN BASALTS OF THE SERRA GERAL GROUP: IMPLICATIONS FOR CARBON STORAGE

THIS IS A NON-PEER-REVIEWED PREPRINT SUBMITTED TO EARTHARXIV. THE PAPER IS UNDERGOING PEER-REVIEW FOR PUBLICATION.

João Paulo G. R. Alves
Institute of Energy and Environment
University of São Paulo
São Paulo, Brazil, 05508-010
joao.guilherme.alves@usp.br

Claudio Riccomini
Institute of Geosciences
Institute of Energy and Environment
University of São Paulo
São Paulo, Brazil, 05508-080
riccomin@usp.br

January 20, 2026

ABSTRACT

Carbon capture and storage (CCS) is an important technology to combat climate change, since it removes carbon dioxide emissions from major industrial sources, helping to reduce greenhouse gas concentrations while the world transitions to cleaner energy systems. In the implementation of CCS projects, petrophysical properties are crucial in determining the most suitable sites to store the CO_2. Therefore, this study applies machine learning techniques to forecast petrophysical properties (density, porosity, and permeability) in the basalts of the Serra Geral Group of the Paraná Basin, located in the State of Santa Catarina, Brazil. By applying machine learning algorithms (XGBoost, Gradient Boosting, and Random Forest) to 28 well log datasets, this research aims to overcome the limitations of traditional empirical methods that often fail to capture the complex variabilities in basalt formations and thereby determine the most suitable locations and sections for carbon storage. The applied machine learning models demonstrated considerable improvements in predictive performance compared to empirical methods from the literature, demonstrating the potential of machine learning to enhance the feasibility and reliability of CCS in basaltic formations. Furthermore, the interpolation of the well data indicated that the northern region of the Serra Geral Group in the State of Santa Catarina exhibits optimal conditions for geological storage. From 600 to 900 m, the basalts present suitable intervals ranging from 10 to 22 m thick, with density lows of almost 2.2 g/cm³, high peaks of 16.9% porosity, and permeability of 45.7 μD. Overall, this study advances CCS technology by applying machine learning to predict petrophysical properties in basalts with higher precision than traditional empirical methods. This approach provides an effective framework for delineating suitable storage and sealing sections, improving site selection, and cost-effective evaluation for CCS projects in the Paraná Basin.

Keywords: Carbon Capture and Storage · Machine Learning Models · Petrophysics · Basalts

1 Introduction

Carbon capture and storage (CCS) is an important technology to combat climate change by capturing carbon dioxide at the source, storing it underground, and preventing large amounts of CO_2 from reaching the atmosphere (IPCC et al., 2018). Among the existing alternatives for geological storage, basalts stand out due to their unique chemical and physical properties, presenting as a promising option for carbon storage due to their abundance and capacity for carbon mineralization (Cartier, 2020; Snæbjörnsdóttir et al., 2020). These rocks are rich in calcium and magnesium, which

react with carbon dioxide to create minerals that securely sequester CO_2 (Oelkers et al., 2008; Snæbjörnsdóttir et al., 2020).

Notable CCS projects have demonstrated the feasibility and potential of basalt formations for CO_2 storage. In Iceland, the CarbFix project has successfully injected and mineralized CO_2 in basaltic rocks, transforming over 95% of the captured CO_2 into stable minerals in less than two years (Matter et al., 2016; von Strandmann et al., 2019; Snæbjörnsdóttir et al., 2020). Similarly, the Wallula project in the Columbia River flood basalt (USA) has explored the capacity of basalt formations in the State of Washington for long-term CO_2 storage, showing promising results in both CO_2 injection and storage efficiency, with approximately 60% of the CO_2 sequestered via mineralization within two years (McGrail et al., 2017; White et al., 2020). These projects exemplify the successful application of CCS in basalt formations, providing insights and data that can be applied to other regions worldwide.

The basalts of the Serra Geral Group in Brazil constitute a significant and still unexplored potential for CO_2 storage. This extensive basalt formation, part of the Paraná Basin, erupted in the Early Cretaceous (Piccirillo & Melfi, 1988; Renne et al., 1992) and offers a vast geological environment suitable for CCS. The region's geological characteristics, including its thickness, density, porosity, permeability, and mineral composition, make it a promising candidate for CO_2 injection and mineralization (Nardy et al., 2008; Rossetti et al., 2019). Due to its volume, it may be considered one of the largest magmatic provinces potentially favorable for carbon fixation on Earth. Laboratory experiments with basalts from this region revealed facilitated, rapid carbonate precipitation beginning 72 hours post-injection, achieving an estimated CO_2 storage of approximately 75% based on the availability of calcium, with carbonate precipitation comprising aragonite (75.9%), dolomite (19.6%), and calcite (4.6%) (Ferreira et al., 2024). Exploring the CCS potential of the Serra Geral basalts could significantly contribute to Brazil's carbon reduction efforts and provide a model for similar formations globally.

1.1 Machine learning applications across different lithologies

Machine learning (ML) algorithms have been successfully used in oil and gas exploration for predicting petrophysical properties across various geological formations due to their ability to handle large datasets and complex relationships. For instance, in sandstones and arenites reservoirs, Farouk et al. (2021) applied neural networks (NN) and least squares support vector machines (LS-SVM) to estimate permeability from core sample data in Egypt. Consequently thsese models performed exceptionally well compared to conventional methods, providing more accurate and reliable permeability predictions. Expanding to sand shale formations, Manzoor et al. (2023) evaluated the efficacy and reliability of LS-SVM, random forest regressor (RFR), extra tree regressor (ETR), gradient boosting regressor (GBR), and decision tree classifier (DTC) in well log data in Pakistan. The high correlation results showed that the application of algorithms provided a cost-effective and robust approach for modern formation evaluation with minimal uncertainty and resource efficiency.

Carbonate reservoirs, characterized for their heterogeneous and intricate pore structures, have particularly benefited from ML applications. Nguyen-Sy et al. (2021) demonstrated the effectiveness of the extreme gradient boosting (XGB) algorithm for sonic velocity prediction using porosity and other petrophysical properties as input parameters, significantly outperforming other machine learning algorithms such as artificial neural networks (ANN) and support vector machines (SVM) with an R-squared of 0.96 and a root mean squared error of 3%. Similarly, Kalule et al. (2023) further demonstrated the advantages of stacked ensemble machine learning methods for predicting porosity and absolute permeability in carbonate rock samples, highlighting improvements in predictive accuracy and model generalizability. Notwithstanding, Zhang et al. (2020) applied the long short-term memory neural network (LSTM) model to predict the shear wave velocity in carbonates. The LSTM model presented an accuracy of 98.9%, whereas the traditional method had only 73%.

Shale formations, characterized by their complex properties and anisotropic nature, have also seen substantial improvements in petrophysical predictions through the application of machine learning. Bennani et al. (2025) estimated the shale porosity of the Sichuan Basin in Western China by applying SVM, multilayer perceptron, and random forest in different ranges of the data. In this case, the random forest model obtained the highest correlation and low root mean squared error, demonstrating the model's suitability for managing limited and complex datasets.

Despite the previous examples of machine learning applications for regression. ML in petrophysics is also applied for different tasks, such as classification (lithofacies, faults, zones, etc.) and clustering. Even with the increase in applications in different scenarios and tasks, the usage of machine learning algorithms in basaltic rocks is still very incipient, relying on empirical models such as linear regression, polynomial fits, and theoretical equations.

1.2 Basaltic formations and machine learning

Machine learning methods have been increasingly applied across various geological settings to model petrophysical properties. However, their application in basaltic formations remains limited, in part due to the intrinsic complexity of these rocks. Basalts are characterized by heterogeneous textures, including vesicular zones, fractured intervals, and layered flow units with variable porosity and permeability. These features arise from dynamic emplacement processes and post-emplacement alterations such as weathering and mineral infilling, making empirical modeling approaches particularly challenging (Navarro et al., 2020; Rossetti et al., 2019). Traditional methods, such as porosity-permeability correlations based on sonic velocity or linear regression models, often fail to capture this complexity, resulting in unreliable predictions when extrapolated to new geological contexts (Breiman, 2001b; Navarro et al., 2020; Rossetti et al., 2019).

Understanding and accurately forecasting petrophysical properties (density, porosity, and permeability) is critical for assessing the feasibility and safety of carbon dioxide (CO_2) storage in basalt formations (McGrail et al., 2011; Zakharova et al., 2012). The variability in these properties across basalt flow units, and even within individual flows, requires modeling strategies that can generalize beyond the original data distribution while preserving local heterogeneities. Advanced ML techniques offer a powerful alternative to empirical approaches by learning complex, nonlinear relationships and accommodating multivariate data structures.

In this context, the present study applies machine learning models to improve the prediction of key petrophysical parameters in the Serra Geral Group basalts of the Paraná Basin in southern Brazil. By leveraging core and well log data, we aim to generate more accurate property maps to support the identification of favorable CO_2 injection zones. This methodological approach contributes to ongoing efforts to advance the understanding of carbon capture and storage (CCS) potential in basaltic formations, offering a replicable framework for similar geological settings worldwide.

2 Material and Methods

2.1 Study area

Identifying regions and sections suitable for carbon capture and storage is crucial for mitigating climate change. This study focuses on the basalts of the Serra Geral Group, located in the western portion of the State of Santa Catarina (Figure 1). These basaltic rocks exhibit significant compositional variations (Nardy et al., 2008; Wildner et al., 2014) and are situated near stationary sources that could benefit from carbon storage (Ketzer et al., 2016). Additionally, the area has a good coverage of wells with petrophysical data (ANP-SGB, 2023), making it an ideal candidate for prospective research.

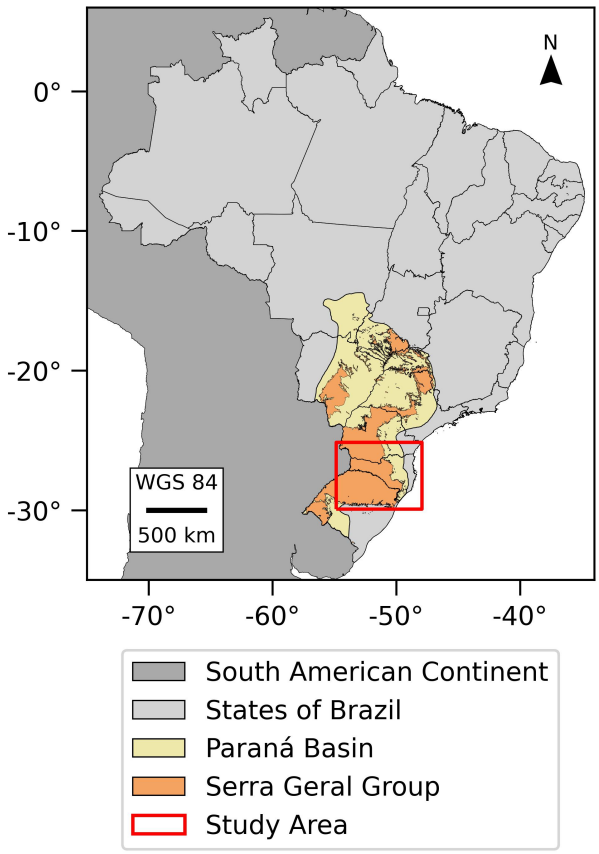

Figure 1: Location map of the study area. The focus is on the basaltic rocks in the Serra Geral Group area at the Paraná Basin in the State of Santa Catarina.

However, due to the intrinsic heterogeneity and variability of petrophysical properties of basalts, empirical equations used to predict the petrophysical properties of basalts have considerable limitations. They typically use a single property as input and can be less flexible than machine learning approaches. These equations may perform poorly with new, unseen data, especially if it deviates from the assumed data distribution and comes from different regions (Breiman, 2001b).

In the following subsections, we describe the application of machine learning techniques to predict density, porosity, and permeability in the study area's basaltic rocks.

2.2 Model Selection and Comparison

To identify the most suitable algorithms for predicting petrophysical properties in basalts, we tested ten machine learning models using consistent evaluation metrics and cross-validation procedures. The comparative analysis included a selection of common regression algorithms, chosen for their ability to handle various data complexities and relationships: Linear Regression, Ridge Regression, Lasso Regression, Support Vector Regression (SVR), Decision Tree Regressor, Random Forest Regressor, Gradient Boosting Regressor, XGBoost Regressor, Bagging Regressor, and Extra Trees Regressor.

The evaluation framework employed a train-test split (80-20) and k-fold cross-validation to ensure robust performance assessment. We used Root Mean Square Error (RMSE), Mean Absolute Error (MAE), and coefficient of determination (R^2) as evaluation metrics. Each model underwent hyperparameter optimization, performing consistent cross-validation folds to certify a fair comparison.

To assess the statistical significance of performance differences between models, we applied the Friedman test, a non-parametric statistical test suitable for comparing multiple algorithms across multiple cross-validation folds (Demšar, 2006). When the Friedman test indicated significant differences ($p < 0.05$), we conducted the Nemenyi post-hoc test to

perform pairwise comparisons between models. Models were then grouped based on their statistical similarity to the best performer: models in Group A showed no statistically significant difference from the top-performing model ($p > 0.05$), while models in Group B demonstrated significantly lower performance. This statistical grouping approach allowed us to identify not only the single best performer but also other models that achieved comparable results, providing a more robust basis for model selection.

For density prediction (Table 1), the Friedman test confirmed statistically significant differences among model performances ($\chi^2 = 44.302$, $p < 0.001$), followed by the Nemenyi post-hoc test for pairwise comparisons. XGBoost achieved the highest accuracy with an RMSE of 0.052, MAE of 0.035, and R^2 of 0.926, closely followed by Gradient Boosting with an RMSE of 0.052, MAE of 0.036, and R^2 of 0.926. In contrast, traditional approaches such as Linear Regression ($R^2 = 0.790$) and Lasso Regression ($R^2 = 0.784$) demonstrated considerably lower performance, thereby showing the complexity of the density-property relationships in basalts.

Table 1: Performance comparison of machine learning models for density prediction.

Model	RMSE	MAE	R^2	Group
Lasso	0.089	0.067	0.784	B
LinearRegression	0.088	0.066	0.790	B
Ridge	0.088	0.066	0.790	B
ExtraTreeRegressor	0.070	0.047	0.868	A
SVR	0.064	0.042	0.887	A
DecisionTreeRegressor	0.063	0.040	0.893	A
RandomForestRegressor	0.061	0.041	0.899	A
BaggingRegressor	0.054	0.036	0.921	A
GradientBoostingRegressor	0.052	0.036	0.926	A
XGBRegressor	0.052	0.035	0.926	A

The porosity prediction models showed different relative performances (Table 2). The Friedman test indicated statistically significant differences among models ($\chi^2 = 20.487$, $p = 0.015$), followed by the Nemenyi post-hoc test for pairwise comparisons. Notably, all models were classified as Group A, indicating that no model was statistically significantly different from the best performer when compared pairwise. This apparent inconsistency reflects the limited statistical power of the pairwise comparisons with the relatively small dataset ($n = 175$ samples), while the Friedman test detected significant differences between other model pairs in the overall ranking. Bagging Regressor demonstrated the best metrics (RMSE = 0.163, MAE = 0.119, $R^2 = 0.822$), however, we selected Gradient Boosting (RMSE = 0.167, MAE = 0.120, $R^2 = 0.813$) for the final porosity model because it belonged to the same statistical performance group (Group A) as the top performer and exhibited superior learning curves with better generalization characteristics. SVR and Linear Regression also displayed comparable effectiveness with R^2 values of 0.816 and 0.812, respectively. This pattern suggests that porosity relationships may follow more linear trends compared to density.

Table 2: Performance comparison of machine learning models for porosity prediction.

Model	RMSE	MAE	R^2	Group
ExtraTreeRegressor	0.210	0.150	0.704	A
DecisionTreeRegressor	0.204	0.145	0.721	A
XGBRegressor	0.180	0.141	0.782	A
Lasso	0.180	0.141	0.784	A
RandomForestRegressor	0.177	0.126	0.789	A
Ridge	0.168	0.123	0.811	A
LinearRegression	0.168	0.123	0.812	A
GradientBoostingRegressor	0.167	0.120	0.813	A
SVR	0.166	0.122	0.816	A
BaggingRegressor	0.163	0.119	0.822	A

For permeability prediction, Random Forest demonstrated the most robust raw performance among the tested algorithms (Table 3). However, the Friedman test revealed no statistically significant differences among model performances (χ^2 = 14.640, p = 0.101), indicating that multiple models achieved comparable predictive accuracy for this property. Due to the inherent complexity and heterogeneity of permeability in basalts, the model achieved moderate but consistent results with an RMSE of 0.386, MAE of 0.299, and R^2 of 0.661. The performance metrics reflect the challenging nature of permeability prediction in basaltic formations, where microscale features and fracture networks influence fluid flow properties.

Table 3: Performance comparison of machine learning models for permeability prediction.

Model	RMSE	MAE	R^2
ExtraTreeRegressor	0.705	0.433	-0.134
DecisionTreeRegressor	0.623	0.390	0.117
Lasso	0.622	0.404	0.120
SVR	0.596	0.373	0.190
LinearRegression	0.552	0.432	0.305
Ridge	0.529	0.365	0.361
XGBRegressor	0.529	0.354	0.362
BaggingRegressor	0.449	0.353	0.541
GradientBoostingRegressor	0.446	0.337	0.548
RandomForestRegressor	0.386	0.299	0.661

The effectiveness of tree-based ensemble methods in this context stems from their capacity to capture complex patterns in heterogeneous basalt formations. These algorithms can model non-linear relationships and feature interactions, essential characteristics when dealing with geological data. The differing performance patterns in density, porosity, and permeability predictions justified our approach of selecting specific algorithms for each property instead of using a one-size-fits-all solution.

2.3 Density model

Previous works applied p-wave velocity (Vp) to predict density, employing linear to second-degree equations (e.g. X. Chen et al. (2015); Rossetti et al. (2019); Vedanti et al. (2018)). In this work, we applied four variables as input in an XGBoost model to predict density: sonic velocity (DT or Vp), gamma ray (GR), spontaneous potential (SP), and induction log deep resistivity (ILD).

Sonic velocity is directly related to density in basalts, where higher velocities typically indicate higher densities due to lower porosity. GR logs reflect natural radioactivity, and variations help identify altered basalt zones, with higher GR

values corresponding to lower density (Queiroz et al., 2024). SP shows limited response in igneous rocks, but altered or mineralized areas may display higher SP readings, signaling density variations (Hutchinson et al., 2007). ILD readings are higher in fresh basalts with greater density, while lower ILD values mark more porous, altered regions and low density (Oliveira et al., 2022).

The XGBoost, or Extreme Gradient Boosting, is an advanced implementation of gradient boosting algorithms designed for speed and performance. It constructs an ensemble of decision trees sequentially, where each subsequent tree is built to correct the errors of the previous trees. This is achieved through an additive model, where new trees are added to minimize a loss function. XGBoost incorporates regularization terms to prevent overfitting and uses decision tree pruning and parallel processing to enhance efficiency. This makes it particularly well-suited for handling large datasets with complex relationships and managing linear and nonlinear interactions among the input features (T. Chen & Guestrin, 2016).

To supply the model, we used freely available wireline log data, inherently co-located on a common depth reference, from the REATE database (ANP-SGB, 2023). Data from 3 wells (14463 samples) containing the curves of DT, GR, SP, ILD, and density (RHOB) were used (Figure 2). Subsequently, the model was applied to 25 additional wells in the study area.

To ensure the reliability of our model, several preprocessing and validation steps were implemented (Figure 3). Outliers were identified and treated to prevent skewed predictions. The dataset was split into training and testing sets, with 20% of the data reserved for testing to evaluate model performance (Geron, 2019). We applied scaling to stabilize variance and make the data more Gaussian-like. Model validation was conducted using K-fold cross-validation (k=5) to ensure the model generalizes well to unseen data (Anguita et al., 2009; James et al., 2023).

Hyperparameter tuning was performed using a randomized search over a parameter grid (Bergstra & Bengio, 2012; Pedregosa et al., 2011), including 'n_estimators', 'learning_rate', 'subsample', 'gamma', 'max_depth', 'min_child_weight', 'reg_alpha', and 'reg_lambda' to optimize model performance. These hyperparameters play distinct roles in the model: n_estimators controls how many sequential trees are built, learning_rate adjusts each tree's contribution to the prediction, subsample governs the fraction of data sampled for each boosting round, gamma specifies the minimum loss reduction required for further partitioning, max_depth limits the complexity of individual trees, and min_child_weight sets the minimum sum of weights in a child node. Additionally, reg_alpha and reg_lambda add L1 and L2 regularization for controlling overfitting and promoting generalization.

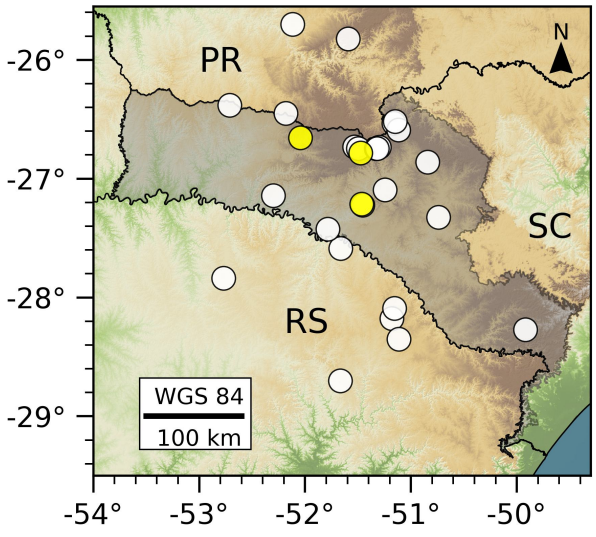

Figure 2: Location map of the 28 wells where the machine learning models were applied to predict the petrophysical properties of basalts and then used to create the interpolated maps. The wells in yellow were used to train-test the density models. The yellow wells are the only ones in the area with density curves.

2.4 Porosity model

Previous works used the relationship between Vp or density to predict porosity, employing linear to exponential equations (e.g. Al-Harthi et al. (1999); X. Chen et al. (2015); Navarro et al. (2020); Rossetti et al. (2019); Vedanti et al. (2018)). Based on tests with bagging and boosting models, we used the Gradient Boosting model to predict porosity using Vp and density as inputs.

Gradient boosting is an ensemble learning technique that builds a model sequentially. It trains a series of weak learners, such as decision trees, where each new tree corrects the errors of the previous ones. The process starts with an initial prediction, and subsequent models are fitted to the residuals of the previous predictions, gradually improving the overall model performance. This results in a robust predictive model that captures complex patterns in the data (Friedman, 2001; Geron, 2019; James et al., 2023).

The porosity model was supplied with data (175 samples) containing Vp, density, and porosity from Rossetti et al. (2019), Goulart (2019), and Famelli (2020). The preprocessing and validation steps were similar to those applied to the density model (Figure 3). Hyperparameter tuning was conducted using a randomized search (k=10) over a defined parameter grid (Bergstra & Bengio, 2012; Pedregosa et al., 2011), including 'n_estimators,' 'learning_rate,' 'max_depth,' 'min_samples_split,' and 'min_samples_leaf.'

These hyperparameters serve specific functions in the model: n_estimators defines how many boosting stages are performed, learning_rate moderates the step size for each stage, max_depth constrains the depth of the decision trees, while min_samples_split and min_samples_leaf regulate the minimum number of samples required to split a node and to be at a leaf node, respectively, helping balance bias and variance in the final model. After hyperparameter tuning, the optimized mode was applied to 28 wells in the study area.

2.5 Permeability model

For permeability, previous empirical equations explored exponential relationships between porosity and permeability to predict data (e.g. Lamur et al. (2017); Mueller et al. (2005); Navarro et al. (2020); Yokoyama and Takeuchi (2009)). Based on the tests, we used the Random Forest model to predict permeability, using Vp, density, and porosity, and a feature was created using Vp multiplied by density squared as inputs.

Random Forest is an ensemble learning method that constructs multiple decision trees during training and outputs the mean prediction of the individual trees. Each tree is built from a random subset of the training data using a bootstrap aggregating or bagging technique. Additionally, random forests select random subsets of features at each split in the decision tree. This randomization reduces the variance of the model, leading to better generalization of unseen data. Aggregating multiple trees helps mitigate overfitting and improves the model's robustness (Breiman, 2001a; Geron, 2019; James et al., 2023).

The permeability model was supplied with Vp, density, porosity, and permeability data (130 samples) from Rossetti et al. (2019) and Famelli (2020). Further preprocessing and validation steps were applied, including cross-validation (k=10), which provided a balanced assessment of the model's generalizability and performance stability across different subsets of the data (Figure 3) (Geron, 2019; James et al., 2023).

Hyperparameter tuning was performed using a grid search strategy over a defined parameter grid (Bergstra & Bengio, 2012; Pedregosa et al., 2011), including 'n_estimators,' 'max_features,' 'max_depth,' 'min_samples_split,' and 'min_samples_leaf.' In the Random Forest model, these hyperparameters control different aspects of the ensemble: n_estimators indicates the number of trees built in the ensemble, max_features specifies how many features are considered at each split, max_depth restricts the maximum depth of the trees to prevent overfitting, and both min_samples_split and min_samples_leaf set the minimum number of samples needed to create splits or be at leaf nodes, thus controlling the model's complexity and robustness. This systematic search allowed us to identify the optimal combination of parameters, maximizing the model's predictive performance for permeability. Subsequently, the model was applied to 28 wells in the study area.

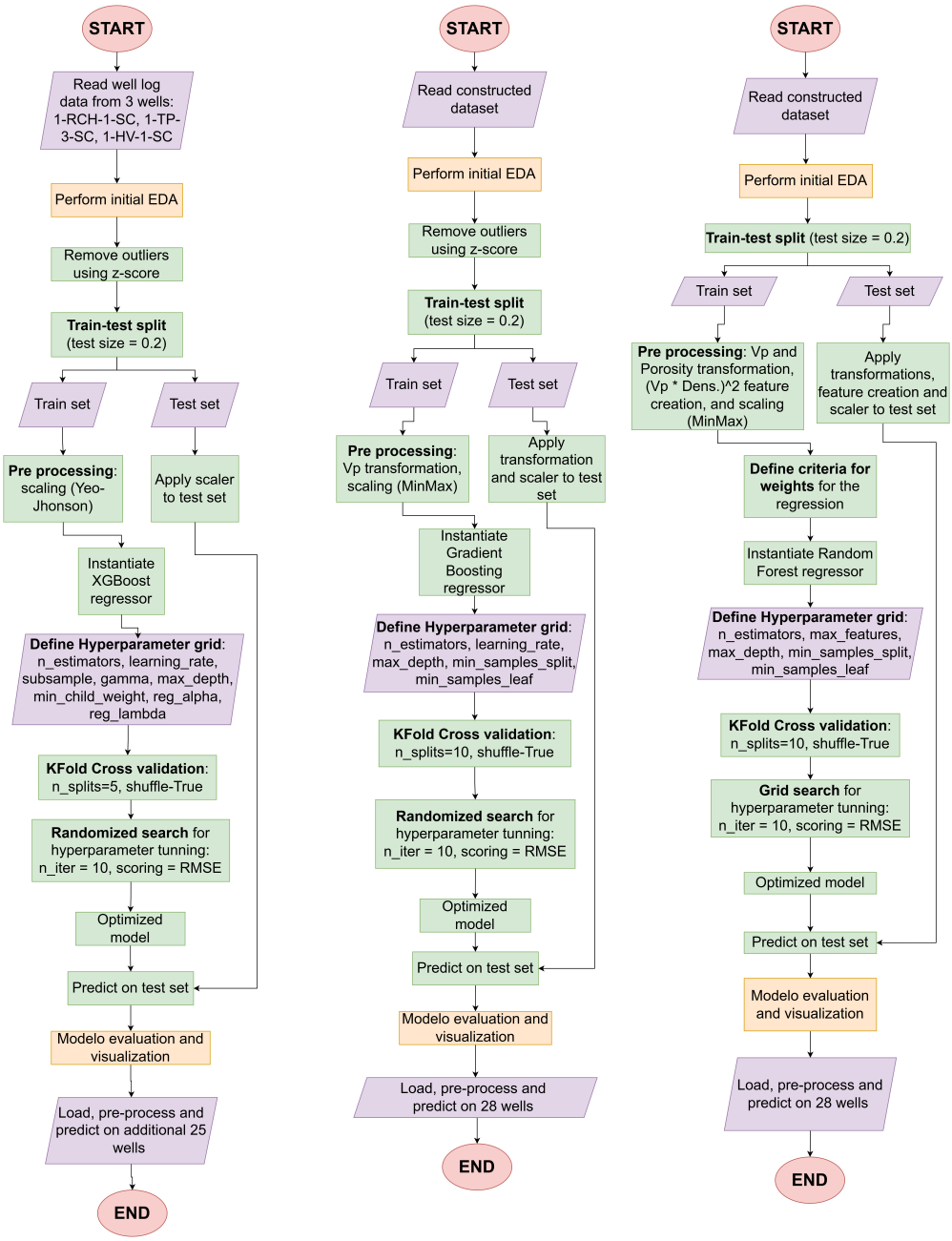

Figure 3: Workflow for machine learning-based prediction of density, porosity, and permeability in basalts from 28 wells in the Paraná Basin.

2.6 Models' performance evaluation

To evaluate the performance of the regression models, we used three metrics: coefficient of determination (R^2), Root Mean Squared Error (RMSE), and Mean Absolute Error (MAE). The coefficient of determination (R^2) (Eq. 1) measures the proportion of variance in the dependent variable explained by the model:

$$R^2 = 1 - \frac{\sum_{i=1}^{n}(y_i - \hat{y}_i)^2}{\sum_{i=1}^{n}(y_i - \bar{y})^2} \tag{1}$$

Where y_i represents the actual values, $\hat{y}_i$ the predicted values, $\bar{y}$ the mean of the actual values, and n represents the number of observations. Root Mean Squared Error (RMSE) (Eq. 2) quantifies the average magnitude of prediction errors:

$$\mathrm{RMSE} = \sqrt{\frac{1}{n}\sum_{i=1}^{n}(y_i - \hat{y}_i)^2} \tag{2}$$

Mean Absolute Error (MAE) (Eq. 3) represents the average absolute difference between predicted and actual values:

$$\mathrm{MAE} = \frac{1}{n}\sum_{i=1}^{n}|y_i - \hat{y}_i| \tag{3}$$

To complete the analysis, the learning curves were analyzed to assess model convergence, overfitting, and generalization capability across training and validation sets. SHAP values (SHapley Additive exPlanations) were used to interpret the predictions made by the machine learning models. SHAP uses a game-theoretic approach to measure each input variable's contribution to the outcome (Lundberg & Lee, 2017). Additionally, residual plots were created to evaluate the quality of the model's outputs.

2.7 Models' application

To identify the most suitable sections in the basalts of the Serra Geral Group for carbon storage, the models were applied to the 28 wells in the study area. All well-logging curves were plotted together, focusing on areas with low density and high porosity and permeability. To delineate the most suitable areas, the average values of each petrophysical property were interpolated using regularized splines with tension in GRASS GIS (Cell size = 500 m, Tension = 20) (Team, 2023; Mitášová & Mitáš, 1993; Mitášová & Hofierka, 1993).

3 Results

3.1 Performance of the machine learning models

This study employs advanced machine learning models to analyze key geological parameters critical for carbon capture and storage in the Serra Geral Group basalts at the Paraná Basin. The models evaluated include XGBoost, Gradient Boosting, and Random Forest, each tested for their predictive accuracy and influence of input features.

Figure 4 presents the results of the XGBoost model applied to estimate the density. The bar graph illustrates the mean SHAP values, quantifying the impact of the features on the model's predictions. The P-Wave velocity (Vp) shows the highest mean SHAP value of 0.15, indicating its significant influence on the model's output. Vp had three times more impact on the model's output than the other inputs combined, suggesting that Vp is a critical predictor in the geological dataset.

In Figure 4b, the high value of the Pearson correlation coefficient (R^2) of 0.94, along with low values of RMSE (0.05) and MAE (0.03), indicates that the model achieves an excellent level of accuracy in predicting the density of the basalts. The residuals plot in Figure 4c helps assess the prediction variance, showing a cloud of points centered around the zero line (dashed orange). This distribution suggests that the residuals are relatively small and randomly dispersed, implying that the model's predictions are consistent across different data points without systematic errors. Figure 4d shows the learning curves, where the convergence of training and cross-validation scores indicates good model generalization and adequate dataset size for reliable predictions.

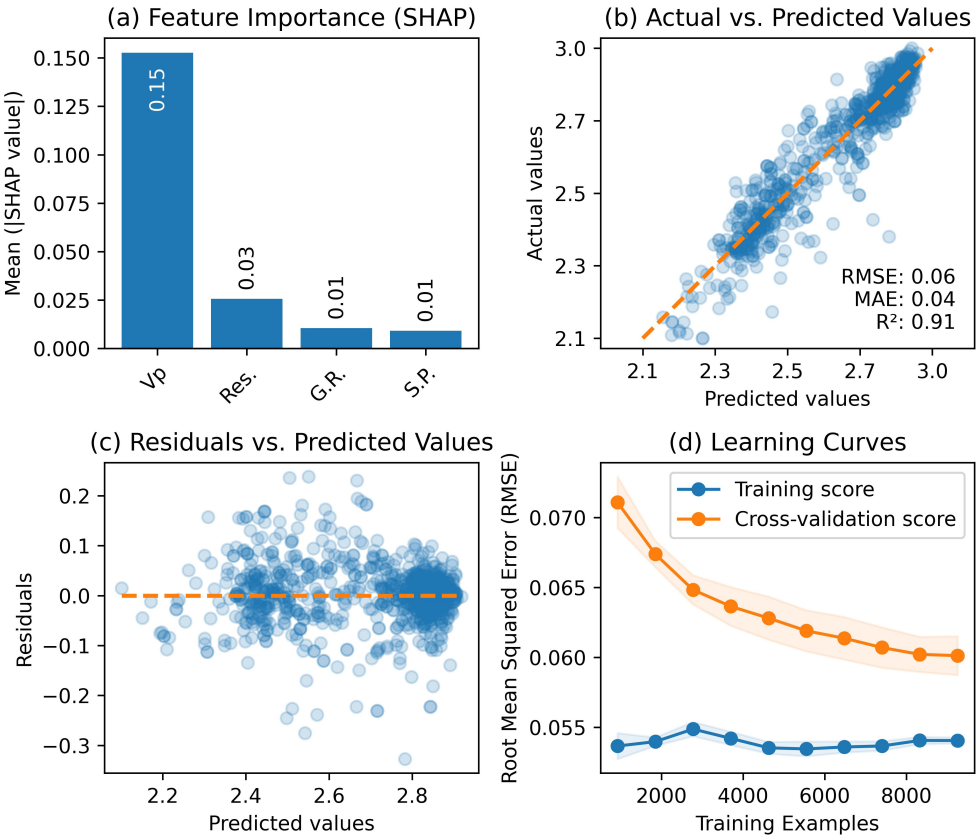

Figure 4: Performance of the XGBoost model used to predict the density of the basalts from the Serra Geral Group. (a) Illustrates the mean SHAP values of input variables. (b) Illustrates the correlation between the predicted and actual values. (c) Residuals plot to assess the variance in predictions. (d) Learning curves.

The application of the equations proposed by X. Chen et al. (2015), Rossetti et al. (2019), and Vedanti et al. (2018) to the test set yielded lower results than those achieved by the XGBoost model (Table 4). The R^2 values from the empirical equations ranged from -0.63 to 0.65. Meanwhile, the RMSE and MAE varied from 0.25 to 0.11 and from 0.21 to 0.09, respectively.

Table 4: Performance comparison of XGBoost model against models from literature.

Model	RMSE	MAE	R^2
X. Chen et al. (2015)	0.25	0.21	-0.63
Vedanti et al. (2018)	0.12	0.09	0.56
Rossetti et al. (2019)	0.11	0.09	0.65
XGBoost Model	0.06	0.04	0.91

Figure 5 details the performance outcomes of the Gradient Boosting model applied to predict porosity. As in the previous model, the Vp represents the highest impact (SHAP value of 0.25), while the density has a lower impact with a SHAP value of 0.08 (Figure 5a). Although slightly lower than the XGBoost model, the Gradient Boosting model maintains a consistent accuracy, as reflected in the regression metrics (Figure 5b). In Figure 5c, the even distribution of residuals around zero suggests that the model's errors are random rather than systematic, validating the model's generalization ability across various data points. The learning curves in Figure 5d demonstrate good model convergence, with both training and cross-validation scores stabilizing and converging, indicating adequate generalization without overfitting despite the limited dataset size.

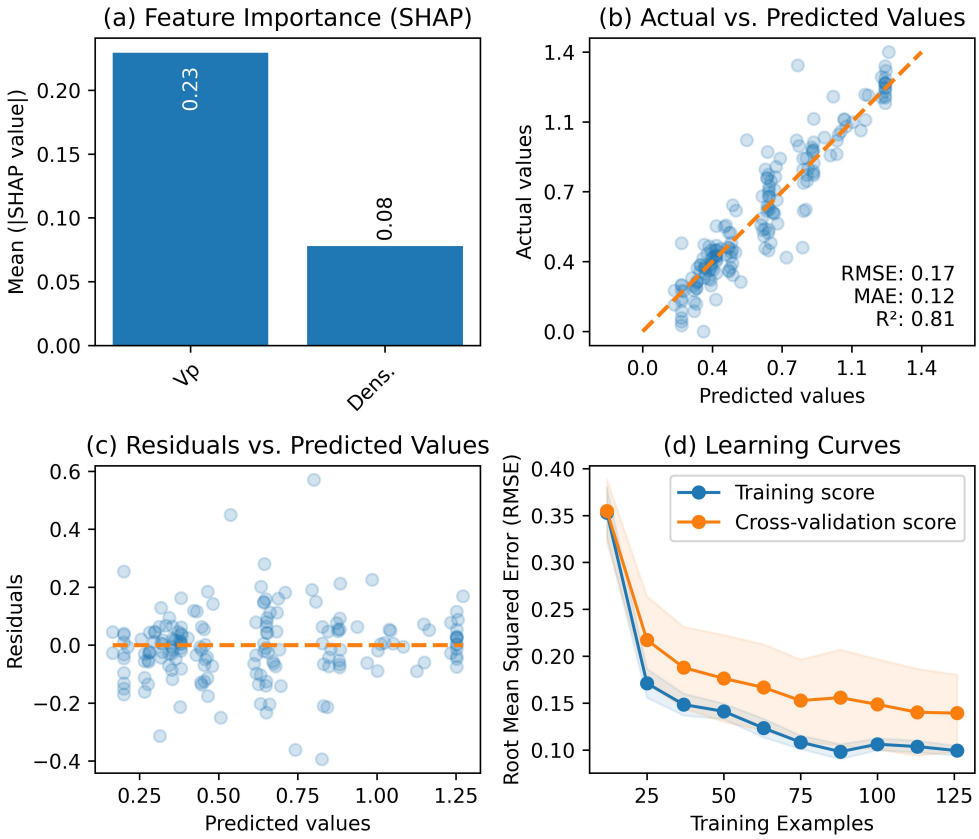

Figure 5: Performance of the Gradient Boosting model used to predict the porosity of the basalts from the Serra Geral Group. (a) Mean SHAP values of input variables. (b) Predicted versus actual values graph. (c) Residuals plot to assess the variance in predictions. (d) Learning curves.

The application of the equations proposed by Al-Harthi et al. (1999), X. Chen et al. (2015), Navarro et al. (2020), Rossetti et al. (2019), and Vedanti et al. (2018) to the test set yielded lower results than those achieved by the Gradient Boosting model (Table 5). The R^2 values from the empirical equations ranged from -1.74 to 0.49. Meanwhile, the RMSE and MAE varied from 11.36 to 4.51 and from 9.94 to 3.77, respectively.

Table 5: Performance comparison of Gradient Boosting model against models from literature.

Model	RMSE	MAE	R^2
Al-Harthi et al. (1999)	11.36	9.94	-1.74
X. Chen et al. (2015)	8.39	4.81	-0.49
Rossetti et al. (2019)	5.36	4.02	0.39
Navarro et al. (2020)	4.91	3.86	0.49
Vedanti et al. (2018)	4.51	3.77	0.57
Gradient Boosting Model	0.06	0.04	0.91

Figure 6 details the performance of the Random Forest model applied to predict permeability in basalts. Unlike previous models, all four input features significantly influence the model's output. The interaction term between Vp and density has the lowest impact (0.03), indicating that while the individual features are influential, their interaction provides additional but lesser predictive power.

The scatter plot (Figure 6b) indicates a moderate correlation between predicted and actual values, as reflected in its metrics, making this a model with weaker predictive power when compared to previous models. The residuals plot

(Figure 6c) shows a concentration of residuals around zero, albeit with a wider spread than observed in the earlier figures. Figure 6d shows the learning curves, where the persistent gap between training and cross-validation scores reflects the challenges of permeability prediction with limited training data, though both curves stabilize, suggesting the model has reached its capacity with the available dataset. These results are due to the intrinsic difficulty in modeling permeability in basalts and the quality and quantity of samples available in the literature that were used to train the model. An improvement in these points can possibly help in modeling the complexity of this problem and result in greater predictive power.

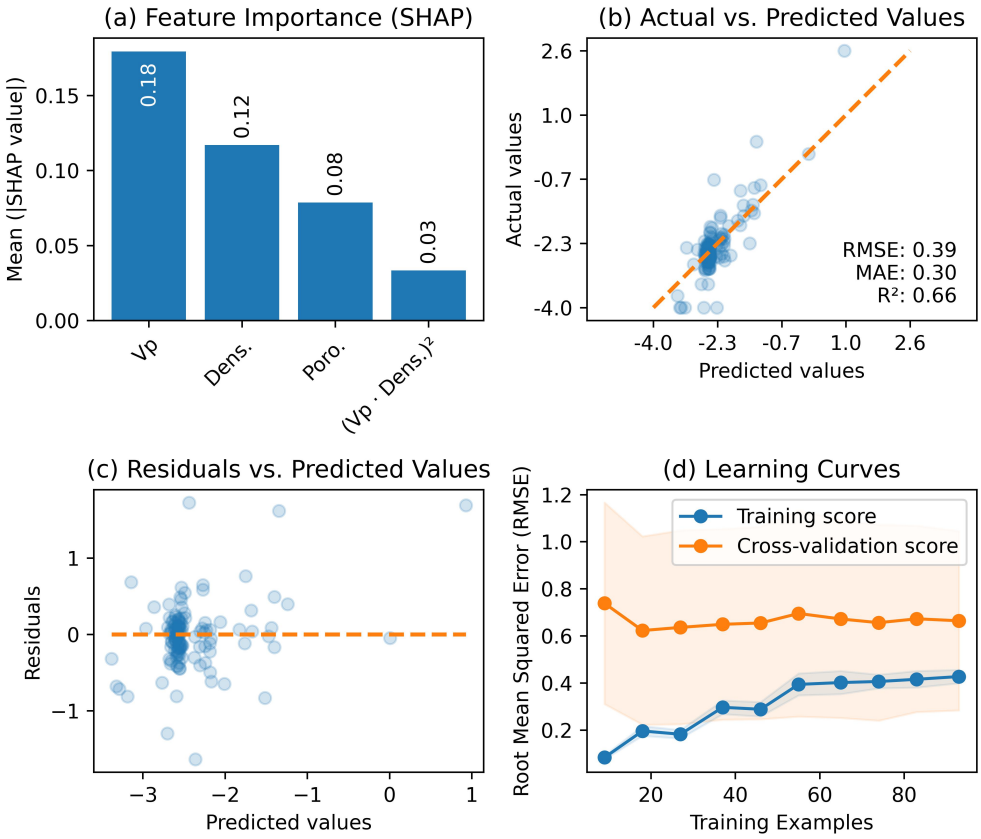

Figure 6: Performance of the Random Forest model used to predict the permeability of the basalts from the Serra Geral Group. (a) Mean SHAP values of input variables. (b) Predicted versus actual values graph. (c) Residuals plot to assess the variance in predictions. (d) Learning curves.

The application of the equations proposed by Lamur et al. (2017), Mueller et al. (2005), Navarro et al. (2020) and Yokoyama and Takeuchi (2009) to the test set yielded significantly poorer results than those achieved by the Random Forest model (Table 6). The R^2 values from the empirical equations were all -0.05 in all cases. Meanwhile, the RMSE and MAE varied from 178.49 to 178.37 and from 39.66 to 39.61, respectively.

Table 6: Performance comparison of Random Forest model against models from literature.

Model	RMSE	MAE	R^2
Yokoyama and Takeuchi (2009)	178.49	39.66	-0.05
Navarro et al. (2020)	178.47	39.65	-0.05
Mueller et al. (2005)	178.44	39.64	-0.05
Lamur et al. (2017)	178.37	39.61	-0.05
Random Forest Model	0.39	0.3	0.66

The results of the three machine learning models show that the P-wave velocity (Vp) is the most impactful input feature, especially for the density and porosity models. The permeability model had moderate results due to the complex nature of the problem. The porosity model had fewer input features but still performed well. The density model performed the best among the models due to its direct correlation with Vp and a large amount of data for training.

3.2 Interpolated maps

The machine learning models were applied to 28 exploratory wells available in the area. Figure 7 presents the interpolated maps of the density, porosity, and permeability of the basalts from the Serra Geral Group in Santa Catarina State, Brazil.

In Figure 7a, the density map demonstrates notable density gradients, particularly in the southern part of the area, indicating possible subsurface heterogeneities. The areas with high density in the southern part correlate to areas with low porosity and permeability. Maps in figures 7b and 7c indicate areas of higher porosity and permeability in the northern part, suggesting more permeable zones with higher carbon storage capacity.

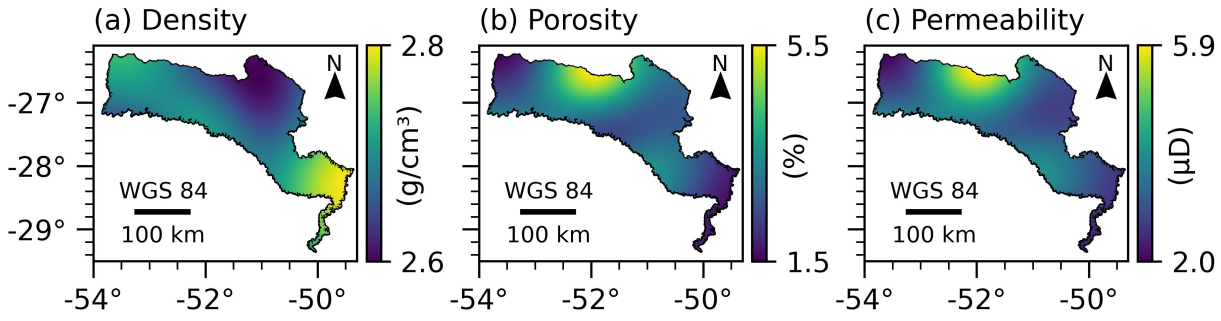

Figure 7: Interpolated maps of petrophysical properties of basalts generated from the application of machine learning models in 28 exploratory wells. (a) Density map. (b) Porosity map. (c) Permeability map. All three maps were interpolated in GRASS-GIS using regularized splines with tension (Cell size = 500 m, Tension = 20).

3.3 Logging curves sections

The basaltic rocks from the Serra Geral Group present variations in their properties and internal fractures, generating sections more suitable for geological storage than others. Figure 8 presents the well logging curves from the exploratory well located in the high porosity and permeability part of the maps presented previously. The well log identified as 1-RCH-1-SC contains a basalt section from the Serra Geral group with 978 m thickness, and with average values of 2.69 g/cm³ for density, 6.54% for porosity, and 6.22 μD for permeability. The section from 600 to 900 m deep was plotted below.

The highlighted sections in grey represent intervals deemed most suitable for carbon capture and storage based on integrating the log data. From 600 to 900 meters, the most suitable intervals vary from 10 to 22 m thick, with density lows of almost 2.2 g/cm³, high peaks of 16.9% apparent porosity, and 45.7 μD permeability. These intervals exhibit a combination of favorable porosity, permeability, and other geophysical properties, suggesting they are optimal targets for further investigation and potential implementation of carbon storage solutions.

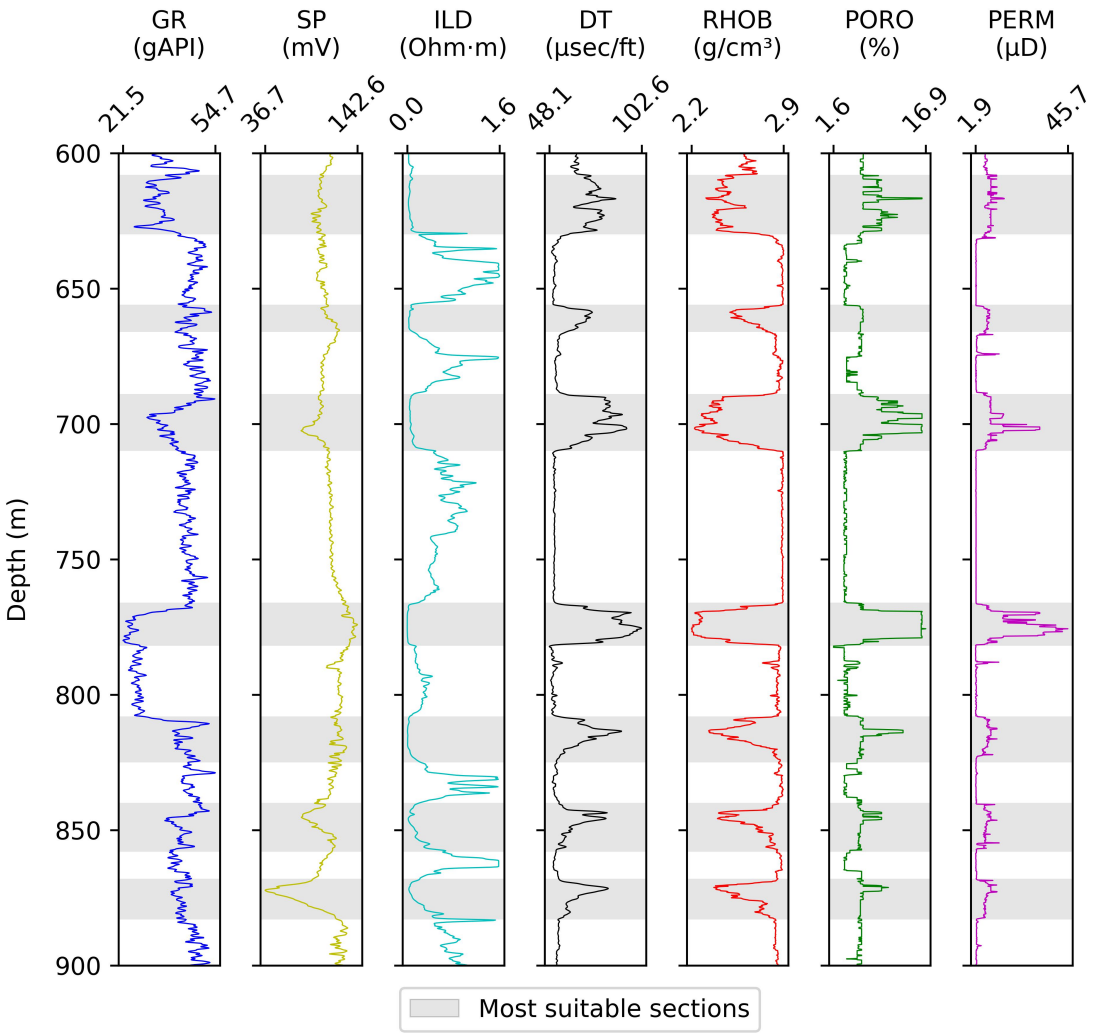

Figure 8: Borehole curves of 1-RCH-1-SC located in a region with high porosity and permeability basalts. Curve names: GR – Gamma Ray, SP - Spontaneous Potential, ILD – Induction Log Deep resistivity, DT – Sonic Velocity, RHOB – Bulk Density, PORO – Porosity, and PERM – Permeability. The most suitable sections for geological storage are highlighted in grey.

4 Discussion

By applying more robust solutions (more input features, advanced algorithms, train-test split, and cross-validation) and training the models only with data from basaltic rocks from the Serra Geral Group, the models presented more satisfactory results than other solutions available in the literature that use more classical statistical solutions and data from different places in the world. The significant improvement in prediction performance, particularly evident in the density model ($R^2 = 0.91$) compared to previous empirical approaches (R^2 ranging from -0.63 to 0.65), demonstrates the advantage of using region-specific data and machine learning techniques for petrophysical property prediction.

The consistent dominance of P-wave velocity (Vp) as a predictor across all models, indicated by SHAP values of 0.15, 0.23, and 0.18 for density, porosity, and permeability, respectively, aligns with the physical relationships between these properties in basaltic rocks. This relationship suggests that seismic data could serve as a cost-effective preliminary screening tool for identifying potential storage zones in future projects, reducing the need for extensive initial drilling campaigns.

The northern region of Santa Catarina's State has the best petrophysical properties for geological storage in basalts; however, due to the low population density in the area (most of the population of the state is concentrated in the coastal

region), the area may not have enough stationary sources to make a project of this magnitude economically feasible (Ketzer et al., 2016). The optimal zones identified in our study, with density lows of 2.2 g/cm³, porosity peaks of 16.9%, and permeability of 45.7 micro-Darcy, are comparable to successful CCS projects in basalts worldwide. For instance, these values align favorably with the CarbFix project in Iceland, where similar properties led to over 95% CO_2 mineralization within two years.

The logging curves display a cyclic pattern that correlates with different flow characteristics. Specifically, they show low density, high porosity, and high permeability in the top and bottom flows, which can be considered potential reservoirs. In contrast, the interiors of massive flows exhibit high density and low porosity-permeability, making them potential caprocks. Similar patterns are observed in the Columbia River flood basalts (Zakharova et al., 2012). The top and bottom flows are typically associated with vesicular and fractured basalts, whereas the interior flows are characterized by massive, less fractured basalts (Guidicini & de Oliveira Campos, 1968).

The thickness variation of suitable intervals (10-22 m) identified in our study presents both opportunities and challenges for CCS implementation. While these intervals provide sufficient volume for storage, their variability requires careful injection strategy planning. The cyclic nature of the flows, evident in the well log data (Figure 8), suggests that multiple storage-seal pairs exist within the same vertical sequence, potentially allowing for staged injection approaches that could optimize storage capacity while maintaining security.

Economic feasibility analysis for CCS projects in the region would need to consider several factors beyond just the technical storage potential. These include transportation infrastructure development costs, proximity to CO_2 sources, monitoring requirements, and potential carbon credit revenues. Future studies should focus on detailed economic modeling incorporating these factors, as well as investigating potential synergies with other industrial activities in the region to improve project viability.

5 Conclusions

The success of carbon sequestration in basalts depends heavily on accessing regions with favorable physical properties for mineralization to occur. Predicting basaltic rocks' density, porosity, and permeability is complex, considering their nonlinear relationships and the challenge of obtaining representative data from specific regions.

The three machine learning models developed in this study demonstrated exceptional predictive capabilities, with the density model achieving an R^2 of 0.91, the porosity model reaching 0.81, and the permeability model attaining 0.66. These results significantly surpass the performance of traditional empirical equations, validating our approach of using region-specific data and advanced algorithms. The strong influence of P-wave velocity across all models suggests its potential as a primary screening tool for future storage site assessment.

The northern region of Santa Catarina's State presented optimal predicted properties, with density lows of 2.2 g/cm³, porosities up to 16.9%, and permeabilities reaching 45.7 micro-Darcy. These characteristics, comparable to successful international CCS projects, indicate promising storage potential. However, the southeast region, despite its proximity to stationary sources, showed less favorable conditions. The identified cyclic pattern of seal-reservoir pairs in the basalt flows provides multiple storage options within single well locations, offering flexibility for injection strategies.

The maps and borehole profiles presented here provide a foundation for future CCS project planning in Brazil, potentially reducing exploration costs and timeline. The developed methodology and models demonstrate broader applicability beyond carbon storage, offering valuable tools for hydrogeological studies and resource exploration throughout the Serra Geral Group at the Paraná Basin. Future work should focus on economic feasibility studies incorporating infrastructure development costs and potential carbon credit revenues to advance CCS implementation in the region.

6 Acknowledgments

The authors are grateful for the financial support from the Human Resources Program of the National Agency of Petroleum, Natural Gas, and Biofuels (PRH-ANP), supported with resources coming from the investment of qualified oil companies in the R&D Clause of ANP Resolution No. 918/2023 (PRH 33.1 - Regarding the announcement No. 1/2018/PRH-ANP; FINEP/FUSP/USP Agreement Ref. 0443/19). C. Riccomini is funded by the Research Productivity Grant #307471/2022-5 of CNPq-Brazil.

7 Code availability

The code for the machine learning models, along with the data used for training, testing, and map interpolation, is available on GitHub and Zenodo. This repository, titled "Application of machine learning methods to forecast petrophysical properties in basalts of the Serra Geral Group: Implications for carbon storage", is licensed under the MIT License and was developed by João Paulo Alves. For inquiries, please contact João Paulo Alves at joao.guilherme.alves@usp.br. The repository was first made available in 2024 and requires a platform to run a Jupyter Notebook, as the code is written in Python. The GitHub repository is avaliable at `https://github.com/jp-alves/ml_basalts_ccs`, and the Zenodo repository can be accessed at `https://doi.org/10.5281/zenodo.13821458`.

References

Al-Harthi, A. A., Al-Amri, R. M., & Shehata, W. M. (1999). *The porosity and engineering properties of vesicular basalt in saudi arabia* (Vol. 54).

Anguita, D., Ghio, A., Ridella, S., & Sterpi, D. (2009). K-fold cross validation for error rate estimate in support vector machines. In *International conference on data mining.* Retrieved from `https://api.semanticscholar.org/CorpusID:11101468`

ANP-SGB. (2023, 10). *Programa de revitalização da atividade de exploração e produção de petróleo e gás natural em Áreas terrestres.*

Bennani, R., Wang, M., Wang, X., & Li, T. (2025). Porosity estimation using machine learning approaches for shale reservoirs: A case study of the lianggaoshan formation, sichuan basin, western china. *Journal of Applied Geophysics*, *237*, 105702. Retrieved from `https://doi.org/10.1016/j.jappgeo.2025.105702` doi: doi:10.1016/j.jappgeo.2025.105702

Bergstra, J., & Bengio, Y. (2012). *Random search for hyper-parameter optimization* (Vol. 13). Retrieved from `http://scikit-learn.sourceforge.net.`

Breiman, L. (2001a). Random forests. *Machine Learning*, *45*, 5-32. Retrieved from `https://doi.org/10.1023/A:1010933404324` doi: doi:10.1023/A:1010933404324

Breiman, L. (2001b). *Statistical modeling: The two cultures* (Vol. 16).

Cartier, K. (2020). Basalts turn carbon into stone for permanent storage. *Eos*, *101*.

Chen, T., & Guestrin, C. (2016, 8). Xgboost: A scalable tree boosting system. In *Proceedings of the acm sigkdd international conference on knowledge discovery and data mining* (p. 785-794). Association for Computing Machinery. doi: doi:10.1145/2939672.2939785

Chen, X., Schmitt, D. R., Kessler, J. A., Evans, J., Coordinated, R. K. A., Schmitt, D., & Boroumand, N. (2015, 5). Empirical relations between ultrasonic p-wave velocity, porosity and uniaxial compressive strength. *RECORDER*, *40*. Retrieved from `https://csegrecorder.com/articles/view/empirical-relations-between-ultrasonic-p-wave-velocity-porosity-and-uniaxia`

Demšar, J. (2006). Statistical comparisons of classifiers over multiple data sets. *Journal of Machine learning research*, *7*(Jan), 1–30.

Famelli, N. (2020). *Associação de litofácies, interação lava-sedimento e caracterização sísmica do magmatismo serra geral na região de uberlândia e araguari (mg)* (Doctoral dissertation, Universidade Federal do Rio Grande do Sul). Retrieved from `http://hdl.handle.net/10183/223773`

Farouk, S., Sen, S., Ganguli, S. S., Abuseda, H., & Debnath, A. (2021). Petrophysical assessment and permeability modeling utilizing core data and machine learning approaches – a study from the badr el din-1 field, egypt. *Marine and Petroleum Geology*, *133*, 105265. Retrieved from `https://doi.org/10.1016/j.marpetgeo.2021.105265` doi: doi:10.1016/j.marpetgeo.2021.105265

Ferreira, A., Santos, R. V., de Almeida, T. S., Camargo, M. A., Filho, J. A., Miranda, C. R., ... Capistrano, G. G. (2024, 12). Unraveling the rapid co2 mineralization experiment using the paraná flood basalts of south america. *Scientific Reports*, *14*. doi: doi:10.1038/s41598-024-58729-w

Friedman, J. H. (2001). *Greedy function approximation: A gradient boosting machine* (Vol. 29).

Geron, A. (2019). *Hands-on machine learning with scikit-learn, keras, and tensorflow : concepts, tools, and techniques to build intelligent systems* (Second edition. ed.). O'Reilly.

Goulart, D. (2019, 12). *Análise e correlação de propriedades físicas e mecânicas de rochas da formação botucatu e grupo serra geral* (Tech. Rep.). Universidade Federal de Santa Catarina. Retrieved from `https://repositorio.ufsc.br/handle/123456789/204071`

Guidicini, G., & de Oliveira Campos, J. (1968). Notas sobre a morfogênese dos derrames basálticos. *Boletim da Sociedade Brasileira de Geologia*, *17*, 15-28.

Hutchinson, P. J., Stockdale, E. G., Charlton, J. E., & Benitez, R. J. (2007). Electric log analysis of precambrian igneous and metamorphic rocks in the st. francois mountians, missouri. In *Symposium on the application of geophysics to engineering and environmental problems 2007* (pp. 1218–1225).

IPCC, Masson-Delmotte, V., Zhai, P., Pörtner, H.-O., Roberts, D., Skea, J., ... Tabatabaei, M. (2018). *Global warming of 1.5°c. an ipcc special report on the impacts of global warming of 1.5°c above pre-industrial levels and related global greenhouse gas emission pathways, in the context of strengthening the global response to the threat of climate change, sustainable development, and efforts to eradicate poverty*. doi: doi:10.1017/9781009157940

James, G., Witten, D., Hastie, T., Tibshirani, R., & Taylor, J. E. (2023). *An introduction to statistical learning: with applications in python*. Springer.

Kalule, R., Abderrahmane, H. A., Alameri, W., & Sassi, M. (2023). Stacked ensemble machine learning for porosity and absolute permeability prediction of carbonate rock plugs. *Scientific Reports*, *13*, 1-17. Retrieved from https://doi.org/10.1038/s41598-023-36096-2 doi: doi:10.1038/s41598-023-36096-2

Ketzer, J. M. M., Machado, C. X., Rockett, G. C., & Iglesias, R. S. (2016). *Atlas brasileiro de captura e armazenamento geológico de co2*. EDIPUCRS. Retrieved from https://www.globalccsinstitute.com/archive/hub/publications/202033/atlas-brasileiro.pdf

Lamur, A., Kendrick, J. E., Eggertsson, G. H., Wall, R. J., Ashworth, J. D., & Lavallée, Y. (2017, 12). The permeability of fractured rocks in pressurised volcanic and geothermal systems. *Scientific Reports*, *7*. doi: doi:10.1038/s41598-017-05460-4

Lundberg, S. M., & Lee, S.-I. (2017). A unified approach to interpreting model predictions. In I. Guyon et al. (Eds.), *Advances in neural information processing systems* (Vol. 30). Curran Associates, Inc. Retrieved from https://proceedings.neurips.cc/paper_files/paper/2017/file/8a20a8621978632d76c43dfd28b67767-Paper.pdf

Manzoor, U., Ehsan, M., Hussain, M., Iftikhar, M. K., Abdelrahman, K., Qadri, S. M., ... Fnais, M. S. (2023). Harnessing advanced machine-learning algorithms for optimized data conditioning and petrophysical analysis of heterogeneous, thin reservoirs. *Energy and Fuels*, *37*, 10218-10234. doi: doi:10.1021/acs.energyfuels.3c01293

Matter, J. M., Stute, M., Snæbjörnsdottir, S., Oelkers, E. H., Gislason, S. R., Aradottir, E. S., ... Broecker, W. S. (2016, 6). Rapid carbon mineralization for permanent disposal of anthropogenic carbon dioxide emissions. *Science*, *352*, 1312-1314. doi: doi:10.1126/science.aad8132

McGrail, B. P., Schaef, H. T., Spane, F. A., Cliff, J. B., Qafoku, O., Horner, J. A., ... Sullivan, C. E. (2017, 1). Field validation of supercritical co2 reactivity with basalts. *Environmental Science and Technology Letters*, *4*, 6-10. doi: doi:10.1021/acs.estlett.6b00387

McGrail, B. P., Spane, F. A., Sullivan, E. C., Bacon, D. H., & Hund, G. (2011). The wallula basalt sequestration pilot project. In *Energy procedia* (Vol. 4, p. 5653-5660). Elsevier Ltd. doi: doi:10.1016/j.egypro.2011.02.557

Mitášová, H., & Hofierka, J. (1993). Interpolation by regularized spline with tension: Ii. application to terrain modeling and surface geometry analysis. *Mathematical Geology*, *25*, 657-669. Retrieved from https://doi.org/10.1007/BF00893172 doi: doi:10.1007/BF00893172

Mitášová, H., & Mitáš, L. (1993). Interpolation by regularized spline with tension: I. theory and implementation. *Mathematical Geology*, *25*, 641-655. Retrieved from https://doi.org/10.1007/BF00893171 doi: doi:10.1007/BF00893171

Mueller, S., Melnik, O., Spieler, O., Scheu, B., & Dingwell, D. B. (2005, 7). Permeability and degassing of dome lavas undergoing rapid decompression: An experimental determination. *Bulletin of Volcanology*, *67*, 526-538. doi: doi:10.1007/s00445-004-0392-4

Nardy, A., Machado, F., & Oliveira, M. (2008, 10). As rochas vulcânicas mesozóicas ácidas da bacia do paraná: litoestratigrafia e considerações geoquímico-estratigráficas. *Brazilian Journal of Geology*, *38*, 178-195. doi: doi:10.25249/0375-7536.2008381178195

Navarro, J., Teramoto, E. H., Engelbrecht, B. Z., & Kiang, C. H. (2020). Assessing hydrofacies and hydraulic properties of basaltic aquifers derived from geophysical logging. *Brazilian Journal of Geology*, *50*. doi: doi:10.1590/2317-4889202020200013

Nguyen-Sy, T., Vu, M. N., Tran-Le, A. D., Tran, B. V., Nguyen, T. T. N., & Nguyen, T. T. (2021). Studying petrophysical properties of micritic limestones using machine learning methods. *Journal of Applied Geophysics*, *184*, 104226. Retrieved from https://doi.org/10.1016/j.jappgeo.2020.104226 doi: doi:10.1016/j.jappgeo.2020.104226

Oelkers, E. H., Gislason, S. R., & Matter, J. (2008, 10). Mineral carbonation of co2. *Elements*, *4*(5), 333-337. Retrieved from https://doi.org/10.2113/gselements.4.5.333 doi: doi:10.2113/gselements.4.5.333

Oliveira, F. V. S. R. S., Gomes, R. T. M., Calonio, L. W., Silva, K. M. S., de Oliveira Carmo, I., Bittencourt, B. T., ... Freire, A. F. M. (2022). Igneability feature: an effective, easy and low-cost way to identify basic igneous rocks using wireline well logs in open hole wells. *Brazilian Journal of Geophysics*, *40*(1), 19–41.

Pedregosa, F., Varoquaux, G., Gramfort, A., Michel, V., Thirion, B., Grisel, O., ... Édouard Duchesnay (2011). Scikit-learn: Machine learning in python. *Journal of Machine Learning Research*, *12*, 2825-2830. Retrieved

from http://jmlr.org/papers/v12/pedregosa11a.html

Piccirillo, E. M., & Melfi, A. J. (1988). *The mesozoic flood volcanism of the paraná basin: Petrogenetic and geophysical aspects*. Universidade de São Paulo, Instituto Astronômico e Geofísico.

Queiroz, B. S., de Castro Valente, S., dos Santos, A. C., & Heilbron, M. (2024). Petrophysical and petrographic data correlation and the discrimination of magmatic environments and processes in santos basin, offshore se brazil. *Journal of South American Earth Sciences*, *147*, 105095.

Renne, P., Ernesto, M., Pacca, I., Coe, R., Glen, J., Prévot, M., & Perrin, M. (1992, 10). The age of parana flood volcanism, rifting of gondwanaland, and the jurassic-cretaceous boundary. *Science (New York, N.Y.)*, *258*, 975-979. doi: doi:10.1126/science.258.5084.975

Rossetti, L. M., Healy, D., Hole, M. J., Millett, J. M., de Lima, E. F., Jerram, D. A., & Rossetti, M. M. (2019, 4). Evaluating petrophysical properties of volcano-sedimentary sequences: A case study in the paraná-etendeka large igneous province. *Marine and Petroleum Geology*, *102*, 638-656. doi: doi:10.1016/j.marpetgeo.2019.01.028

Snæbjörnsdóttir, S., Sigfússon, B., Marieni, C., Goldberg, D., Gislason, S. R., & Oelkers, E. H. (2020, 2). Carbon dioxide storage through mineral carbonation. *Nature Reviews Earth and Environment*, *1*, 90-102. doi: doi:10.1038/s43017-019-0011-8

Team, G. D. (2023). *Geographic resources analysis support system (grass gis) software, version 8.3*. Retrieved from https://grass.osgeo.org doi: doi:10.5281/zenodo.5176030

Vedanti, N., Malkoti, A., Pandey, O. P., & Shrivastava, J. P. (2018, 8). Ultrasonic p- and s-wave attenuation and petrophysical properties of deccan flood basalts, india, as revealed by borehole studies. *Pure and Applied Geophysics*, *175*, 2905-2930. doi: doi:10.1007/s00024-018-1817-x

von Strandmann, P. A. P., Burton, K. W., Snæbjörnsdóttir, S. O., Sigfússon, B., Aradóttir, E. S., Gunnarsson, I., ... Gislason, S. R. (2019, 12). Rapid co2 mineralisation into calcite at the carbfix storage site quantified using calcium isotopes. *Nature Communications*, *10*. doi: doi:10.1038/s41467-019-10003-8

White, S. K., Spane, F. A., Schaef, H. T., Miller, Q. R., White, M. D., Horner, J. A., & McGrail, B. P. (2020, 11). Quantification of co2 mineralization at the wallula basalt pilot project. *Environmental Science and Technology*, *54*, 14609-14616. doi: doi:10.1021/acs.est.0c05142

Wildner, W., Camozzato, E., Toniolo, J. A., Binotto, R. B., Iglesias, C. M. F., & Laux, J. H. (2014). *Mapa geológico do estado de santa catarina.* CPRM. Retrieved from https://rigeo.sgb.gov.br/handle/doc/17996 (Escala 1:500.000. Programa Geologia do Brasil. Subprograma de Cartografia Geológica Regional)

Yokoyama, T., & Takeuchi, S. (2009, 2). Porosimetry of vesicular volcanic products by a water-expulsion method and the relationship of pore characteristics to permeability. *Journal of Geophysical Research: Solid Earth*, *114*. doi: doi:10.1029/2008JB005758

Zakharova, N. V., Goldberg, D. S., Sullivan, E. C., Herron, M. M., & Grau, J. A. (2012, 11). Petrophysical and geochemical properties of columbia river flood basalt: Implications for carbon sequestration. *Geochemistry, Geophysics, Geosystems*, *13*. doi: doi:10.1029/2012GC004305

Zhang, Y., Zhong, H. R., Wu, Z. Y., Zhou, H., & Ma, Q. Y. (2020). Improvement of petrophysical workflow for shear wave velocity prediction based on machine learning methods for complex carbonate reservoirs. *Journal of Petroleum Science and Engineering*, *192*, 107234. Retrieved from https://doi.org/10.1016/j.petrol.2020.107234 doi: doi:10.1016/j.petrol.2020.107234